Nanoscale Res Lett (2008) 3:1–5
DOI 10.1007/s11671-007-9105-1

NANO EXPRESS

Transient Photoinduced Absorption in Ultrathin As-grown Nanocrystalline Silicon Films

Emmanouil Lioudakis · Andreas Othonos · Ch. B. Lioutas · N. Vouroutzis

Received: 21 October 2007 / Accepted: 8 November 2007 / Published online: 27 November 2007
© to the authors 2007

Abstract We have studied ultrafast carrier dynamics in nanocrystalline silicon films with thickness of a few nanometers where boundary-related states and quantum confinement play an important role. Transient non-degenerated photoinduced absorption measurements have been employed to investigate the effects of grain boundaries and quantum confinement on the relaxation dynamics of photogenerated carriers. An observed long initial rise of the photoinduced absorption for the thicker films agrees well with the existence of boundary-related states acting as fast traps. With decreasing the thickness of material, the relaxation dynamics become faster since the density of boundary-related states increases. Furthermore, probing with longer wavelengths we are able to time-resolve optical paths with faster relaxations. This fact is strongly correlated with probing in different points of the first Brillouin zone of the band structure of these materials.

Keywords Ultrafast spectroscopy · Nanoscale silicon thin films

E. Lioudakis (✉) · A. Othonos (✉)
Department of Physics, Research Center of Ultrafast Science, University of Cyprus, P.O. Box 20537, Nicosia 1678, Cyprus
e-mail: mlioud@ucy.ac.cy

A. Othonos
e-mail: othonos@ucy.ac.cy

Ch. B. Lioutas · N. Vouroutzis
Solid State Physics Section, Department of Physics, Aristotle University of Thessaloniki, Thessaloniki 541 24, Greece

Introduction

Polycrystalline silicon thin films have proven to be of major importance in the semiconductor industry [1–4]. It is considered an important component of silicon integrated circuit technology and is currently used in a wide range of device application. Although considerable effort has been carried out in the characterization of this material, little work has been performed on nanoscale film thickness. It is expected that a decrease in the film thickness to nanometer scale results in a modification of the energy states in these nanofilms. This is a result of two factors, one due to the large fraction of boundary-atoms to the total number of atoms and second because the core of the nanograins is transformed due to quantum size effect. Recently, preliminary ultrafast carrier dynamic results in these types of thin films [5] reveal various relaxation mechanisms under different growth conditions. As a consequent, the optical properties of these materials in steady state and photoexcited conditions change considerable providing a more applicable picture of these films in photovoltaic applications [4] and optoelectronic devices. The optical properties in steady state conditions for these materials have been recently published [6]. In that work, we reported on the determination of critical points (CPs) in the first Brillouin zone of the band structure for these films with thickness 5–30 nm using spectroscopic ellipsometry giving an important insight of the effect of the film thickness for the tunability of absorption. Based on the extracted CPs from that work, in this article, we report on a comprehensive study of transient photoinduced absorption (PA) of as-grown nanocrystalline silicon films with thickness ranges of 5–30 nm. From this study, we are able to time-resolve the relaxation paths within their complex energy band structure of the nanocrystalline silicon films. The

influence of the grain boundaries and the quantum confinement effect due to the nanoscale grain size on the relaxation dynamics is examined in detail.

Experimental Procedure

In this work, the dynamical behavior of as-grown nanocrystalline silicon films following ultrashort pulse excitation is investigated through the temporal behavior of reflectivity and transmission [7]. The source of excitation consists of a self mode-locked Ti:Sapphire oscillator generating 100 fs pulses at 800 nm. A chirped pulsed laser amplifier based on a regenerative cavity configuration is used to amplify the pulses to approximately 1 mJ at a repetition rate of 1 kHz. These ultrashort pulses are used in a pump probe setup where the pump beam is frequency doubled at 400 nm using a non-linear crystal. A half wave plate and a polarizer in front of the non-linear crystal were utilized to control the intensity of the pump incident on the sample. A small part of the fundamental energy was also used to generate a super continuum white light by focusing the beam on a sapphire plate. An ultrathin high reflector at 800 nm was used to reject the residual fundamental light from the generated white light to eliminate the possibility of excitation by the probe light. The white light probe beam is used in a non-collinear geometry, in a pump-probe configuration. Optical elements such as focusing mirrors were utilized to minimize dispersion effect and thus broadening of the laser pulse. The reflected and transmission beams are separately directed onto their respective silicon detectors after passing through a bandpass filter selecting the probe wavelength from the white light. The differential reflected and transmission signals were measured using lock-in amplifiers with reference to the optical chopper frequency of the pump beam. The temporal variation in the PA is extracted using the transient reflection and transmission measurements, which is a direct measure of the photoexcited carrier dynamics within the probing region [8]. In this work, optical absorption fluence of ~ 0.5 mJ/cm^2 has been used to excite the nanocrystalline silicon films and determine its temporal behavior. The estimated photogenerated carrier density was approximately 4×10^{19} carriers/cm^3 for the fluence used in this work.

The samples under investigation were very thin as-grown nanocrystalline silicon films with thickness in the range of 5–30 nm fabricated on a quartz substrate using low pressure chemical vapor deposition (LPCVD) of silicon from silane at 610 °C and 300 mTorr. Transmission electron microscopy (TEM) and electron diffraction patterns taken in these nanofilms reveal the crystallinity of them with a grain size that is depended on film thickness. In the z-direction the grain size was approximately equal to film thickness, while in the plane (x–y directions) it was in the range of 5–19 nm in the case of the 5 nm thick film and in the range of 6–32 nm in the case of the 30-nm film [6]. A typical example of our images is shown in Fig. 1 for the cross-sectional specimen of 5, 15, and 30 nm film thickness, respectively.

Results and Discussion

Figure 2 shows the temporal behavior for as-grown nanocrystalline silicon films over a range of 300 ps following excitation at $t = 0$ with 3.1 eV and 100 fs pulses. Here, we should point out that measurements were also carried out at carrier densities up to five times less than the above, and still showed similar relaxation rates with a linear peak signal dependence. The three graphs shown in Fig. 2 depict the typical temporal PA response corresponding to the nanofilms with thickness 5, 15, and 30 nm for various probing wavelengths between 400 and 980 nm. From these results, it is clearly evident the characteristic sharp increase in the absorption followed by a multi-exponential decay

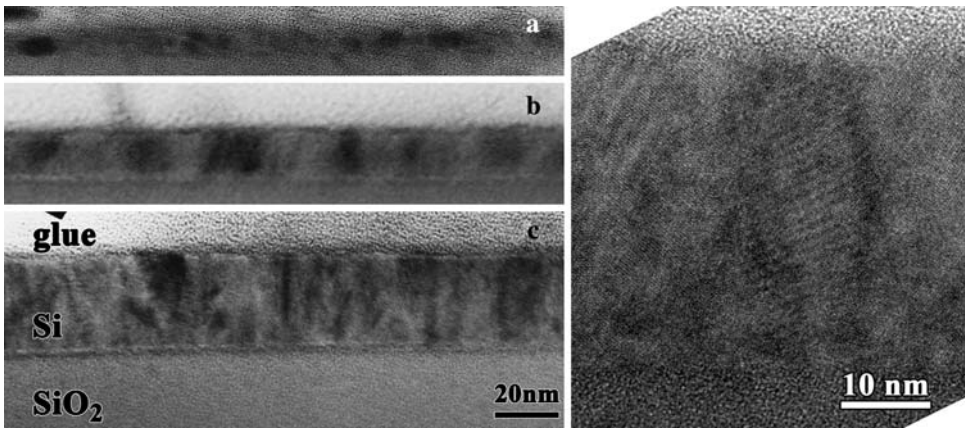

Fig. 1 (*Left*) Bright field images from cross-section specimens from the films with nominal thicknesses: (**a**) 5 nm, (**b**) 15 nm, and (**c**) 30 nm, respectively, revealing the evolution of the columnar structure as the thickness increases. The scale in the (**c**) holds for all the images. The real thicknesses are larger than the nominal ones by about 15%. (*Right*) A high resolution TEM image from the 30-nm film is shown. It is obvious the bigger size of nanocrystals in this case

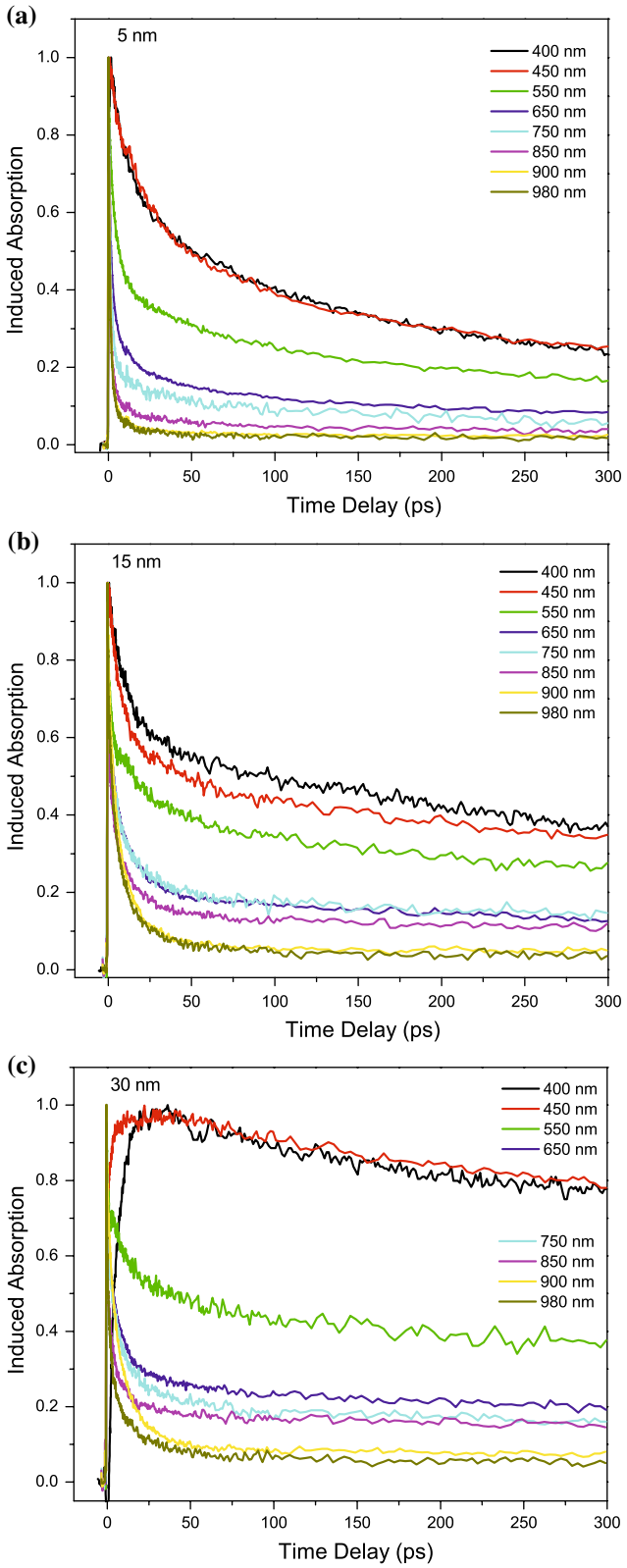

Fig. 2 Normalized transient PA measurements for the nanocrystalline silicon films with thickness (**a**) 5 nm, (**b**) 15 nm, and (**c**) 30 nm. The samples were excited at 3.1 eV and probed at different probing wavelength ranging from 400 to 980 nm

towards the equilibrium. The observed rise time corresponds to the time which the photogenerated carriers need to reach the probing energy states lower to the initial excitation level providing the maximum coupling efficiency which results in the maximum induced change in the absorption.

Close examination of the required rise time (within the first few picoseconds) reveals a variation with film thickness between 5 and 30 nm. A typical example of this behavior is shown in Fig. 3 at 450 nm probing wavelength. For the 5-nm film sample, the rise time is estimated to be 1.2 ps whereas for the films of thickness 10–20 nm the rise time is only 600 fs. In addition, it is interesting to note that further increase of the film thickness causes an increase in the rise time (1.5 ps for 25-nm film). This is more obvious at 30-nm film where the rise time is estimated to be $\sim$25 ps. Based on the extracted CPs [6] this long rise time is attributed to state filling of the occupied surface-related states. This results in a negative contribution to the induced absorption from secondary excitations. Thus, the 25 ps is the estimated time for the photogenerated carriers to move out of these boundary-related states. This result is in agreement with previous degenerated [9] pump-probe measurements where a combination of state filling and PA has been observed at 400 nm with similar delay time at 30-nm film. Here, we should point out that data for the longer probing wavelengths (550–980 nm) show a rise time of approximately 300 fs for all the samples involved in this work.

Figure 3 shows the temporal behavior of the films in the first few picoseconds when probing at 450 nm. It is obvious that with decreasing the film thickness we notice a

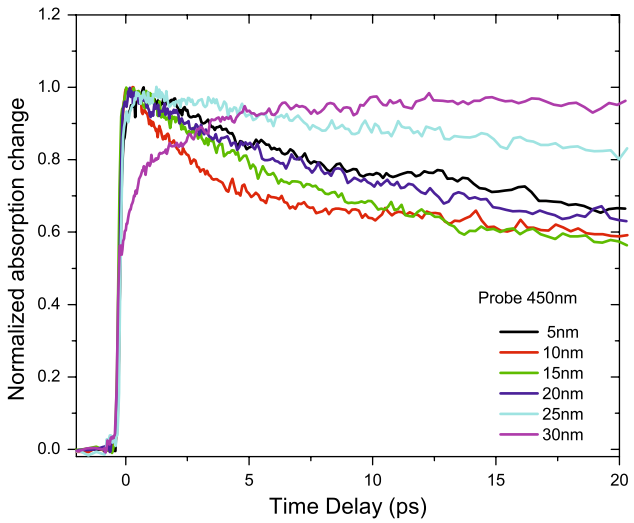

Fig. 3 Normalized transient PA measurements for the nanocrystalline silicon films with thickness varied from 5 to 30 nm. The samples were excited at 3.1 eV and probed at 450 nm (2.75 eV) with 100 fs pulses

faster carrier relaxation recovery in the first few picoseconds. This behavior occurs up to film thickness of 10 nm. A further decrease in the film thickness results in a substantial slower recovery. We believe this may be attributed to the exciton confinement in the surrounding interface of the formed nanograins due to the small thickness of the material. This results in altering the available decay channels of the photogenerated carriers.

With regards to the long time behavior of the films from the data in Fig. 2, one may clearly deduce that the photogenerated carriers have the longest decays at the shortest probing wavelengths. Furthermore, the 30-nm film appears to have the longest recovery compared with the other samples with smaller film thickness. The relaxation dynamics of these nanofilms are rather complex and a fit to the experimental data requires a multi-exponential function. A satisfactory fit ($\chi^2 > 0.99$) has been achieved with a minimum of a three exponential decay function for all the data signifying the multiple recombination channels available for the photogenerated carriers in these materials. The faster recombination components observed for the smaller thickness samples may be attributed to the increase of density of boundary-related states with decreasing film thickness.

For a more quantitative analysis, we present the fitting parameters of the three-exponential decay model in Table 1. From these results, it is obvious that the fast relaxation mechanism becomes more important with increasing probing wavelength for the 5-nm film (see amplitude component represented by parameter-A in Table 1). With increasing probing wavelengths, the decays appear to be faster. This we believe is attributed to different probing regions of the first Brillouin zone of the band structure of these materials. Here, we should point out that the first two decays (τ_1, τ_2) are strongly related with intraband relaxation mechanisms whereas the third slow decay (τ_3) corresponds to the relaxations from states strongly correlated to the band edge of the materials. Furthermore, the observed decays for the 30-nm film at the shortest probing wavelength appear to be very long, which is attributed to the non-radiative relaxation dynamics of this thicker material approaching the bulk behavior of silicon.

Table 1 Fitting parameters obtained from the experimental data of Fig. 2 using a three exponential decay relaxation model

	450 nm	550 nm	650 nm	980 nm
5-nm film				
A	0.12	0.42	0.61	0.72
τ_1	3.15	2.42	1.02	0.72
B	0.43	0.20	0.24	0.24
τ_2	27.20	17.54	9.22	3.78
C	0.44	0.38	0.15	0.04
τ_3	439.55	398.5	330.58	255.48
15-nm film				
A	0.39	0.38	0.33	0.36
τ_1	6.97	1.09	0.44	0.70
B	0.15	0.23	0.46	0.56
τ_2	47.59	21.81	8.66	7.61
C	0.46	0.39	0.21	0.08
τ_3	981.40	709.59	542.46	237.27
30-nm film				
A	0.12	0.27	0.35	0.57
τ_1	137.57	0.45	0.41	0.68
B	0.34	0.25	0.38	0.34
τ_2	1998.83	16.39	8.05	7.27
C	0.54	0.48	0.27	0.09
τ_3	2258.35	968.06	816.28	336.30

Conclusions

We have investigated carrier dynamics in as-grown nanocrystalline silicon film with thickness in the range of 5–30 nm using non-degenerate pump-probe configuration. An observed long initial rise of the PA for the thicker films agrees well with the existence of boundary-related states acting as fast traps. Transient PA measurements reveal information about the relaxation dynamics within the complex band structure of these nanofilms. With decreasing the thickness of material, the relaxation dynamics become faster since the density of boundary-related states increases. Furthermore, probing with longer wavelengths we are able to time-resolve optical paths with faster relaxations. This fact is strongly correlated with probing in different points of the first Brillouin zone of the band structure of these materials.

Acknowledgments The authors would like to thank Dr. A. G. Nassiopoulou from the IMEL/NCSR Demokritos, Athens, Greece for the fabrication of these samples. The work in this article was partially supported by the research programs ERYAN/0506/04 and ERYNE/0506/02 funded by the Cyprus Research Promotion Foundation in Cyprus.

References

1. S. Tiwari, F. Rana, C. Chan, L. Shi, H. Hanafi, Appl. Phys. Lett. **69**, 1232 (1996)
2. R.A. Rao, et al., Solid-State Electron. **49**, 1722 (2005)
3. C. Monzio Compagnoni, D. Ielmini, A.S. Spinelli, A.L. Lacaita, IEEE Trans. Electron Devices **52**, 2473 (2005)
4. M.C. Beard, K.P. Knutsen, P. Yu, J.M. Luther, Q. Song, W.K. Metzger, R.J. Ellingson, A.J. Nozik, Nano Lett. **7**, 2506 (2007)
5. E. Lioudakis, A. Othonos, A.G. Nassiopoulou, Ch.B. Lioutas, N. Frangis, Appl. Phys. Lett. **90**, 191114 (2007)

6. E. Lioudakis, A. Antoniou, A. Othonos, C. Christofides, A.G. Nassiopoulou, Ch.B. Lioutas, N. Frangis, J. Appl. Phys. **102**, 083534 (2007)
7. A. Othonos, J. Appl. Phys. **83**, 1789 (1998)
8. E. Lioudakis, A.G. Nassiopoulou, A. Othonos, Appl. Phys. Lett. **90**, 171103 (2007)
9. E. Lioudakis, A. Othonos, Phys. Status Solidi (RRL) **2**, 19 (2008)